

$P]_2W(CO)_4$  is larger than in  $(C_6H_5O)_3PW(CO)_5$  (480 vs. 411 Hz).<sup>14</sup>

Replacement of carbon monoxide ligands by phosphorus ligands in the series  $LCr(CO)_{6-n}$  will result in a higher electronic density on chromium which will be partially distributed to the remaining carbonyl groups by back-bonding from the filled  $d\pi$  metal orbitals to the empty  $\pi^*$  orbitals of CO; *i.e.*, the chromium-carbon bond order theoretically should increase while the carbon-oxygen bond order (and stretching force constant) should decrease as the negative charge on Cr increases. This phenomenon has been investigated very extensively by infrared analysis<sup>7,8,15</sup> but this present work is the first case in which simple bond length comparisons can be made. The average Cr-C bond length [1.878 (6) Å] in *trans*- $L_2Cr(CO)_4$  is significantly shorter than the average of the four *cis* Cr-C bond lengths<sup>2</sup> [1.896 (4) Å] in  $LCr(CO)_5$ , which in turn is shorter than the mean Cr-C bond length [1.909 (3) Å] in the unsubstituted chromium hexa-

carbonyl.<sup>16</sup> The C-O bond lengths are also in the expected direction for the substituted compounds; *viz.*, in *trans*- $L_2Cr(CO)_4$  the average C-O length [1.140 (8) Å] is larger than that of the average *cis* CO's [1.131 (6) Å] in  $LCr(CO)_5$ ; however, the differences are too small to be statistically significant. In addition the C-O bond length for  $Cr(CO)_6$  is intermediate [1.137 (4) Å] between these two values. Again the standard deviation is large compared to the differences in lengths. It has been pointed out earlier that the C-O bond length is relatively insensitive to bond order,<sup>17</sup> and therefore perhaps it is not surprising that these relatively insignificant differences in C-O bond lengths were obtained.

The geometry of the triphenyl phosphite found in this work is very similar to that found in  $(C_6H_5O)_3PCr(CO)_5$ .<sup>2</sup> Slight differences in the bond angles about phosphorus in these two cases have been discussed elsewhere.<sup>18</sup>

(16) A. Whitaker and J. W. Jeffery, *Acta Crystallogr.*, **23**, 977 (1967).

(17) F. A. Cotton and R. M. Wing *Inorg. Chem.*, **4**, 314 (1965).

(18) S. O. Grim, H. J. Plastas, C. L. Huheey, and J. E. Huheey, *Phosphorus*, **1**, 61 (1971).

(14) P. R. McAllister, Ph.D. Thesis, University of Maryland, 1967.

(15) G. R. Dobson, I. W. Stolz, and R. K. Sheline, *Advan. Inorg. Chem. Radiochem.*, **8**, 1 (1966).

CONTRIBUTION FROM THE SHELL DEVELOPMENT COMPANY,  
OAKLAND, CALIFORNIA 94623

## The Crystal and Molecular Structure of Bis(cyclopentadienyl)-2,2'-bi- $\pi$ -allyl-bis(nickel) $(C_5H_5 \cdot Ni \cdot C_3H_4 - C_3H_4 \cdot Ni \cdot C_5H_5)$

By A. E. SMITH\*

Received April 21, 1971

The structure of bis(cyclopentadienyl)-2,2'-bi- $\pi$ -allyl-bis(nickel)  $(C_5H_5 \cdot Ni \cdot C_3H_4 - C_3H_4 \cdot Ni \cdot C_5H_5)$  has been determined from three dimensional X-ray data collected by counter methods using graphite and LiF monochromatized Mo  $K\alpha$  radiation. The unit cell is monoclinic, space group  $P2_1/n$ ,  $a = 9.934$  (4) Å,  $b = 7.775$  (4) Å,  $c = 9.573$  (4) Å,  $\beta = 110.55$  (10)°, two molecules per unit cell. The calculated and observed densities are 1.570 and  $1.59 \pm 0.04$  g/cm<sup>3</sup>. The structure was refined by full-matrix least-squares to a conventional  $R$  factor on  $F$  of 3.47% and a weighted  $R$  factor of 2.80% for 1387 reflections. The C-C bonds in the cyclopentadienyl ring differ significantly at the  $5\sigma$  level and consist of an "allyl" group with C-C bond distances of 1.398 and 1.394 Å and a "short" bond of 1.401 Å separated by two "long" bonds of 1.438 and 1.423 Å, respectively. The estimated standard deviation of the C-C bonds is 0.006 Å. The partial localization of the bonds in the cyclopentadiene ring can be explained, as suggested by Dahl and Wei<sup>1</sup> and Bennett, *et al.*,<sup>2</sup> in terms of the removal of the cylindrical symmetry around the Ni atom resulting in the removal of the metal orbital degeneracy, which in turn serves to remove the degeneracy of the bonding orbitals of the cyclopentadienyl ring. Results of extended Hückel molecular-orbital calculations on this complex are in agreement with the observed partial localization of the bonds in the cyclopentadienyl ring.

### Introduction

Several crystalline bimetallic  $\pi$ -allyl complexes of nickel and palladium and cyclopentadienyl have been prepared and reported by Keim.<sup>3</sup> Since no structural information was available for these complexes an X-ray investigation was undertaken of a complex whose chemical analysis indicated it to be of composition  $C_5H_5 \cdot Ni \cdot C_3H_4 - C_3H_4 \cdot Pd \cdot C_5H_5$ . It became apparent from the space group and calculated and measured density that the molecule possessed a center of symmetry and was actually  $C_5H_5 \cdot Ni \cdot C_3H_4 - C_3H_4 \cdot Ni \cdot C_5H_5$ . Later,

nmr evidence<sup>3</sup> suggested that a disproportionation had occurred in solution  $2NiPdLn = Ni_2Ln + Pd_2Ln$  ( $Ln = C_{16}H_{18}$ ). Chemical analysis of crystals grown with the X-ray specimen confirmed the composition as  $C_5H_5 \cdot Ni \cdot C_3H_4 - C_3H_4 \cdot Ni \cdot C_5H_5$ .

It was decided however to proceed with the structure determination to establish the molecular configuration of this type of complex. In addition, at the time the structure became of interest, the monochromator for the automatic diffractometer arrived. The crystals of the complex were well suited for checking the Lorentz-polarization corrections for the LiF and graphite monochromator crystals. This required the collection of accurate data sets for the spherical crystal using LiF and graphite monochromatized and Zr-filled Mo  $K\alpha$  radiation. Subsequent comparison of the data sets

\* Present address: 72 San Mateo Rd, Berkeley, Calif. 94707

(1) L. F. Dahl and C. H. Wei, *Inorg. Chem.*, **2**, 713 (1963).

(2) M. J. Bennett, M. R. Churchill, M. Gerloch, and R. Mason, *Nature (London)*, **201**, 1318 (1964).

(3) W. Keim, *Angew. Chem.*, **80**, 968 (1968).

showed that the LiF and graphite data were in good agreement and superior to the Zr-filtered data. The data obtained with the graphite monochromator were more extensive and of higher precision since the intensity was about five times that available with the LiF crystal. As a result, the standard deviation in bond lengths was only  $\sim 1/2$  that obtained with the LiF data. A brief discussion of the comparison of the data sets<sup>4</sup> and the advantages of the use of monochromators are given in the Appendix. The results indicate that the interesting chemical information, *i.e.*, the partial localization of the C-C bonds in the  $C_5H_5$  ring in the asymmetrical complex  $(C_5H_5 \cdot Ni \cdot C_3H_4)_2$ , could not have been established with the Zr-filtered data.

### Collection and Reduction of the Data

Crystals suitable for the X-ray analysis were grown by the slow evaporation of a toluene solution in a stream of dry nitrogen. Selected crystals were ground into spheres and mounted in thin-walled Lindemann glass capillaries with dilute lacquer in a dry nitrogen atmosphere. The spherical crystal used for the collection of the data was  $0.375 \pm 0.006$  mm in diameter.

A series of precession and Weissenberg photographs taken with Ni-filtered Cu  $K\alpha$  radiation showed the crystal to be monoclinic with  $2/m$  Laue symmetry. The systematic extinctions observed were  $h0l$  for  $l$  odd and  $0k0$  for  $k$  odd. These absences are consistent with space groups  $C_{2h}^2-P21/c$ . It was more convenient to describe the structure in terms of space group  $P21/n$ . The unit cell dimensions were measured on a Picker four-circle automatic X-ray diffractometer using Zr-filtered Mo  $K\alpha$  radiation ( $\lambda$  0.71069 Å). Fourteen medium to high angle reflections from the crystal were accurately centered and used for a least-squares refinement of the lattice parameters. The parameters obtained at  $18^\circ$  were  $a = 9.934$  (4) Å,  $b = 7.775$  (4) Å,  $c = 9.573$  (4) Å, and  $\beta = 110.55$  ( $10^\circ$ ). The density calculated for two formula units is  $1.570$  g/cm<sup>3</sup> in good agreement with the observed value  $1.59 \pm 0.04$  g/cm<sup>3</sup>. The cell measurements were made with filtered radiation since the intensity is relatively insensitive to changes in  $\chi$  with the monochromator in the geometrical arrangement used in the Picker diffractometer, particularly with crystals of moderate or large mosaic spread. As a result fairly large uncertainties in the unit cell dimensions can occur if  $\chi$  is included in the least-squares refinement of cell dimensions from data collected with the monochromator.

The spherical crystal used for collecting data was mounted in a thin-walled Lindemann glass capillary with the monoclinic axis along the  $\phi$  axis of the diffractometer to minimize the possibility of multiple reflections. The initial data were collected with a Picker four-circle card-controlled automatic diffractometer, using a LiF monochromator crystal and Mo  $K\alpha$  radiation with a takeoff angle of  $1.5^\circ$ . The intensity from the LiF monochromator crystal was approximately 18% of that available with Zr-filtered radiation. During the collection of the data a graphite monochromator crystal (001 plane) became available and a complete data set was collected with the same crystal of  $(C_5H_5 \cdot Ni \cdot C_3H_4)_2$ . The intensity from the graphite monochromator under the conditions employed was about 85% of that of the Zr-filtered radiation. The mosaic character of the crystal was checked by performing  $\omega$  scans with several reflections. Grinding the crystals into spheres increased their mosaic spread somewhat; the  $\omega$  scan peak width at half maximum height was  $\sim 0.08^\circ$  after grinding.

Intensity data were collected by the  $\theta$ - $2\theta$  scan technique at a scan rate of  $0.5^\circ/\text{min}$ . The scan range was  $-1.00^\circ$  from  $K\alpha_1$  to  $+1.00^\circ$  from the  $2\theta$  value calculated for  $K\alpha_2$ . Stationary-counter, stationary-crystal background counts of 20 sec were taken at each end of the scan range. The scintillation counter was 27 cm from the crystal and had an aperture of  $6 \times 7$  mm. The detector collimator was 1.0 mm in diameter. Molybdenum foil attenuators were inserted automatically when the intensity exceeded about 7000 counts/sec. A standard reflection was monitored every 3-4 hr. There was no variation in their intensity beyond that expected from counting statistics. The mean value of  $F$  for the 42 standard (006) reflections measured was 38.7 electrons with standard deviation of 0.09.

(4) A. E. Smith, American Crystallographic Association Meeting, Tucson, Ariz., 1968, paper H2.

Data were collected up to  $2\theta \approx 65^\circ$ ; there were very few reflections above background beyond  $2\theta \approx 55^\circ$ . The data used for the structure determination were restricted therefore to  $2\theta \leq 60^\circ$ . A fairly large number of very faint reflections were present, however, in this  $2\theta$  range, particularly with the LiF data set. The data were corrected for Lorentz and polarization effects and for absorption. The  $(LP)^{-1}$  factor used for the monochromator in the configuration of the Picker monochromator was

$$(LP)^{-1} = \sin 2\theta \left( \frac{1 + \cos^2 2\theta m}{\cos^2 2\theta + \cos^2 2\theta m} \right)$$

where  $\theta m$  is the Bragg angle setting of the monochromator crystal. The  $2\theta m$  values for the graphite and LiF monochromator crystals were  $11.87^\circ$  and  $20.45^\circ$ , respectively. The linear absorption coefficient  $\mu$  for this complex for Mo  $K\alpha$  radiation is  $26.79$  cm<sup>-1</sup>. An analytical expression of the form

$$\sum_{n=0}^3 A_n (\sin \theta)^n$$

was fitted by least squares to the interpolated value of  $\mu r$  (0.502) for the absorption correction factor  $A^*$  for a sphere.<sup>5</sup> This expression was then used to correct for absorption during the Lorentz-polarization corrections.

Two different weighting schemes were tried, both however gave the same values for the bond distances and only minor differences in the  $R$  factors. Because of the relatively large number of very weak reflections resulting from the relatively high  $2\theta$  scan range, the initial weighting scheme was designed to reduce the weight of those reflections whose intensities were close to background. Those intensities which were  $\leq 5\%$  of the background were given zero weight; if the intensities were greater than 5% and less than 20% of background, their  $\sigma F$ 's were doubled. For the remaining reflections, the  $\sigma F$ 's were taken as

$$\sigma(F) = \frac{[S_1 \sigma(F_0^2)]^{1/2}}{2F_0}$$

where  $S$  is a scale factor. The weighting scheme and expression for  $\sigma(I)$  finally adopted was similar to that of Busing and Levy<sup>6</sup> and that of Corfield, *et al.*,<sup>7</sup> with  $p = 0.02$ . Of the 1539 reflections collected, 1387 with  $I \geq 3\sigma(I)$  were given  $\sigma(F) > 0$ .  $\sigma F$  was taken equal to the expression given above. The final values for  $R$  and  $R_w$  (for 1387 reflections of none zero weight) were 0.034 and 0.027, respectively.

### Structure Determination

The initial phase of the structure determination was carried out with data collected with a LiF monochromator with Mo  $K\alpha$  radiation. The Ni atom and most of the carbon atoms in the cyclopentadienyl ring were located from a three-dimensional Patterson synthesis.<sup>8</sup> A structure factor calculation followed by a difference Fourier synthesis phased by the Ni atoms revealed the position of all the carbon atoms. Full-matrix least-squares refinement was begun and the  $R$  factor decreased from 0.34 to 0.06 in three cycles. Because of the greater intensity available, the data collected with the graphite monochromator were used in the subsequent least-squares refinement. The positional parameters from the LiF data were used as starting values and anisotropic temperature factors were applied.

The function minimized was  $\Sigma w \Delta^2$ , where  $w = 1/\sigma^2(F_0)$  and  $\Delta = |F_o| - |F_c|$ ,  $|F_o|$  and  $|F_c|$  being the observed and calculated structure amplitudes, respectively. The atomic scattering factors were taken from Cromer and Waber's<sup>9</sup> values with the exception that Stewart's, *et al.*,<sup>10</sup> values were used for hydrogen. The anomalous scattering factors for Ni were included

(5) "International Tables for X-ray Crystallography," Vol. II, Kynoch Press, Birmingham, England, 1959, p 302, Table 5.3.6B.

(6) W. R. Busing and H. Levy, *J. Chem. Phys.*, **26**, 563 (1957).

(7) P. W. R. Corfield, R. J. Doedens, and J. A. Ibers, *Inorg. Chem.*, **6**, 197 (1967).

(8) In addition to various local programs, the programs used in refinement were Busing and Levy's ORFLS program, Zalkin's, FORDAP FOURIER, LSLONG least squares, and DISTAN distance and angle programs, and Johnson's ORTEP thermal ellipsoid program. Hope's program HPOSN was used to calculate the hydrogen positions.

(9) D. T. Cromer and J. T. Waber, *Acta Crystallogr.*, **18**, 104 (1965).

(10) R. F. Stewart, E. R. Davidson, and W. T. Simpson, *J. Chem. Phys.*, **42**, 3172 (1965).

in the calculation of the structure factors throughout the refinement. Cromer's<sup>11</sup> values for  $\Delta f'$  and  $\Delta f''$  for Ni were used.

The discrepancy indices  $R$  and  $R_w$  were 0.040 and 0.034, respectively, after two cycles. A difference Fourier synthesis was then calculated and all the hydrogens were readily located quite close to the calculated theoretical positions. A composite difference Fourier map of the hydrogen atoms is shown in Figure 1.

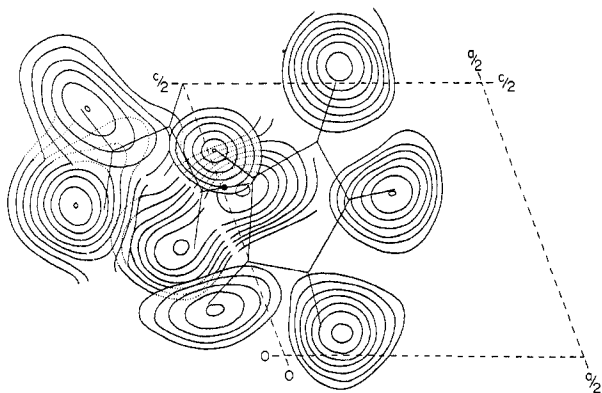


Figure 1.—Composite sections of a difference map indicating the location of hydrogen atoms. The contours are evenly spaced on an arbitrary scale.

TABLE I  
ATOMIC COORDINATES

Atom <sup>a</sup>	<i>x</i>	<i>y</i>	<i>z</i>
Ni	0.00674 (5)	0.18862 (5)	0.30896 (5)
C(1)	-0.0247 (5)	-0.0613 (5)	0.2973 (5)
C(2)	-0.0480 (3)	0.1263 (4)	0.4215 (4)
C(3)	-0.1554 (5)	0.1400 (6)	0.3776 (5)
C(4)	0.0885 (5)	0.2773 (5)	0.1490 (5)
C(5)	-0.0052 (4)	0.4014 (5)	0.1694 (4)
C(6)	0.0566 (5)	0.4492 (5)	0.3241 (5)
C(7)	0.1868 (4)	0.3637 (5)	0.3943 (5)
C(8)	0.2036 (4)	0.2533 (6)	0.2869 (6)
H(1)	0.0508 (35)	-0.1259 (42)	0.3220 (39)
H(2)	-0.1303 (43)	-0.0796 (54)	0.2086 (46)
H(3)	-0.1782 (38)	0.1930 (46)	0.4492 (38)
H(4)	-0.2400 (38)	0.1145 (46)	0.2858 (39)
H(5)	0.0997 (36)	0.2134 (45)	0.0634 (39)
H(6)	-0.1242 (38)	0.4443 (48)	0.0884 (42)
H(7)	0.0271 (42)	0.5303 (50)	0.3759 (43)
H(8)	0.2476 (35)	0.3664 (44)	0.5116 (39)
H(9)	0.2757 (37)	0.1938 (46)	0.3160 (41)

<sup>a</sup> *x*, *y*, *z* are in fractional monoclinic coordinates. The standard deviation of the least significant figure is given in parentheses.

### Description of the Structure

The crystal structure of  $\pi-(C_5H_5 \cdot Ni \cdot C_3H_4)_2$  consists of discretely packed molecules. An inspection of the intermolecular contacts shows there are none appreciable.

TABLE II  
THERMAL PARAMETERS<sup>a</sup>

Atom	$B_{11}$	$B_{22}$	$B_{33}$	$B_{12}$	$B_{13}$	$B_{23}$
Ni	3.11 (2)	2.50 (2)	2.99 (2)	-0.21 (2)	1.15 (1)	0.51 (2)
C(1)	6.99 (32)	2.89 (19)	4.53 (23)	-1.03 (20)	2.44 (24)	0.22 (18)
C(2)	3.14 (17)	2.53 (15)	3.57 (17)	-0.60 (13)	1.40 (14)	0.42 (14)
C(3)	3.20 (21)	5.24 (25)	5.59 (27)	-0.04 (18)	1.81 (20)	2.09 (21)
C(4)	5.82 (25)	4.12 (22)	4.07 (21)	-0.38 (18)	2.95 (19)	0.23 (17)
C(5)	4.73 (21)	3.95 (20)	3.49 (20)	-0.11 (17)	1.66 (17)	1.37 (16)
C(6)	6.35 (26)	2.77 (19)	5.12 (24)	-1.05 (18)	3.34 (22)	0.10 (17)
C(7)	3.82 (20)	3.97 (20)	3.85 (20)	-0.90 (16)	0.65 (16)	0.55 (17)
C(8)	3.26 (21)	4.72 (23)	6.28 (28)	0.42 (18)	2.15 (20)	1.94 (21)
$B^b$						
H(1)	2.6 (0.9)					
H(2)	7.7 (1.2)					
H(3)	3.6 (1.0)					
H(4)	4.5 (1.0)					
H(5)	5.0 (1.0)					
H(6)	6.8 (1.1)					
H(7)	6.2 (1.2)					
H(8)	4.6 (0.9)					
H(9)	4.1 (1.0)					

<sup>a</sup> The standard deviation of the least significant figure is given in parentheses. Anisotropic thermal parameters are in the form  $\exp[-(h^2B_{11} + k^2B_{22} + l^2B_{33} + 2hkB_{12} + 2hlB_{13} + 2klB_{23})]$ . <sup>b</sup>  $B$  is the isotropic thermal parameter in  $\text{\AA}^2$ .

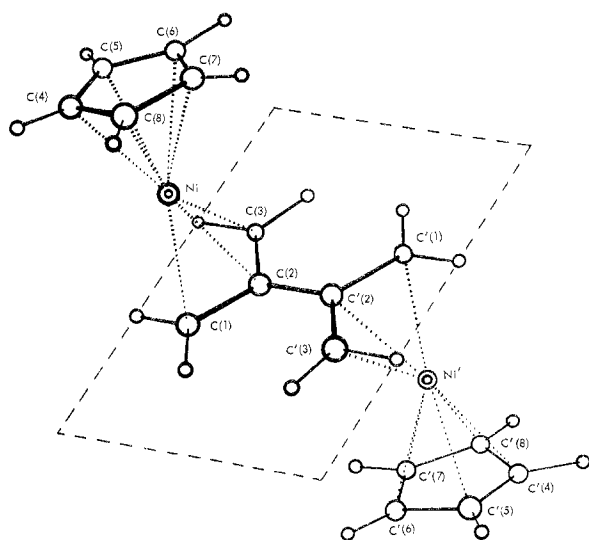
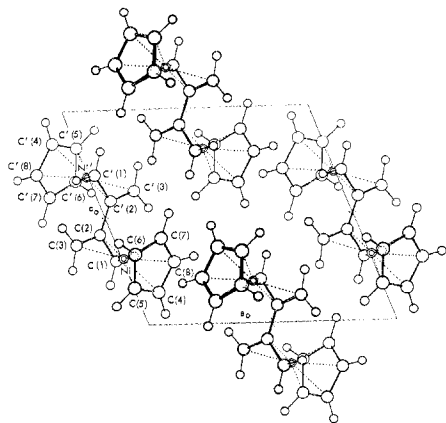
The hydrogen atoms were added to the structure factors using coordinates obtained from the difference maps and two cycles of least squares computed. Isotropic temperature factors were used for the hydrogen atoms and anisotropic factors for the other atoms. The refinement converged with  $R = 0.034$  and  $R_w = 0.027$  (118 variables, 1387 data). No parameter shifted by more than about one-eighth of its standard deviation in the final least squares cycle. The standard deviation of unit weight was 0.97, close to the expected value of unity.

The positional and thermal parameters derived from the last cycle of least-squares are presented in Tables I and II along with the associated standard deviations in these parameters estimated from the inverse matrix. The final values of  $10F_o$  and  $10F_c$  are given in Table III<sup>12</sup> for the 1387 reflections used in the refinement.

(11) D. T. Cromer, *Acta Crystallogr.*, **18**, 17 (1965).

(12) Table III, a listing of structure factor amplitudes, will appear immediately following this article in the microfilm edition of this volume of the journal. Single copies may be obtained from the Reprint Department, ACS Publications, 1155 Sixteenth St., N.W., Washington, D. C. 20036. Remit check or money order for \$3.00 for photocopy or \$2.00 for microfiche.

ciably smaller than the sum of the corresponding van der Waals radii. The shape of the molecule does not appear to be attributable in any significant degree to intermolecular forces. A perspective view of the molecule is shown in Figure 2. The packing arrangement projected along the *b* axis is shown in Figure 3. Principal interatomic distances and angles and their standard deviations computed from the final parameters and the correlation matrix are given in Tables IV and V. The root-mean-square amplitudes of vibration of the atoms are listed in Table VI. The orientations of the thermal ellipsoids are indicated in ORTEP, Figure 4. The directions of maximum vibration of the ring carbon atoms are all approximately normal to the ring-centroid to carbon vectors and in the plane of the ring. Libration of the ring about the Ni-cyclopentadienyl vector probably accounts for the observed thermal motion. The C-C distances in the cyclopentadienyl

Figure 2.—Schematic drawing of  $(C_5H_5 \cdot Ni \cdot C_3H_4)_2$  complex.Figure 3.—Unit cell of  $(C_5H_5 \cdot Ni \cdot C_3H_4)_2$  complex viewed along  $b$  axis.TABLE IV  
PRINCIPAL INTERATOMIC DISTANCES<sup>a</sup>

Atoms	Distance Å	Atoms	Distance, Å
Ni-C(1)	1.965 (4)	C(1)-C(2)	1.411 (6)
Ni-C(2)	1.933 (3)	C(2)-C(3)	1.408 (6)
Ni-C(3)	1.978 (4)	C(4)-C(5)	1.401 (6)
Ni-C(4)	2.087 (4)	C(4)-C(8)	1.423 (6)
Ni-C(5)	2.103 (4)	C(5)-C(6)	1.438 (6)
Ni-C(6)	2.079 (4)	C(6)-C(7)	1.398 (6)
Ni-C(7)	2.167 (4)	C(7)-C(8)	1.394 (6)
Ni-C(8)	2.101 (4)	C(2)-C(2')	1.484 (6)

<sup>a</sup> The standard deviation of the least significant figure is given in parentheses.

TABLE V  
PRINCIPAL BOND ANGLES

Atoms	Angle, deg
C(1)-C(2)-C(3)	111.52 (36)
C(4)-C(5)-C(6)	104.92 (36)
C(5)-C(6)-C(7)	111.12 (37)
C(6)-C(7)-C(8)	105.57 (37)
C(7)-C(8)-C(4)	109.78 (38)
C(8)-C(4)-C(5)	108.50 (37)

ring consist of the two adjacent short distances C(6)-C(7) and C(7)-C(8) of 1.398 (6) and 1.394 (6) Å, respectively, and a short bond C(4)-C(5), 1.401 (6) Å, separated by the two long bonds C(5)-C(6) and C(8)-

TABLE VI<sup>a</sup>

Atom	ROOT MEAN SQUARE AMPLITUDES OF VIBRATION, Å		
	Max	Med	Min
Ni	0.198 (1)	0.195 (1)	0.178 (1)
C(1)	0.298 (6)	0.239 (5)	0.191 (5)
C(2)	0.213 (4)	0.200 (4)	0.179 (4)
C(3)	0.266 (5)	0.258 (5)	0.201 (5)
C(4)	0.271 (5)	0.229 (5)	0.227 (5)
C(5)	0.245 (5)	0.224 (5)	0.210 (5)
C(6)	0.283 (5)	0.255 (5)	0.187 (5)
C(7)	0.224 (5)	0.221 (5)	0.220 (5)
C(8)	0.282 (5)	0.245 (5)	0.203 (5)

<sup>a</sup> The standard deviation of the least significant figure is given in parentheses.

C(4) of lengths 1.438 (6) Å and 1.423 (6) Å, respectively, Figure 5b. Four of the atoms in the cyclopentadienyl ring are planar within experimental error and the fifth carbon atom, C(7) is displaced 0.049 Å from this plane. The equation of the least-squares plane through the four carbon atoms (based on monoclinic coordinates) is  $0.6469X + 0.7233Y - 0.4534Z = 1.485$ . The deviations of the four atoms from this plane are C(4), -0.003; C(5), 0.003; C(6), -0.002; and C(8), 0.002 Å (root mean square deviation 0.003 Å). The distances of these four carbon atoms from the Ni atom are equal within the limit of experimental error and range from 2.079 Å to 2.101 Å with standard deviation of 0.004 Å. Carbon atom C(7) is at a significantly greater distance from the Ni at 2.167 (4) Å.

The C-C bonds in the allyl portion of the bis-allyl molecule are equal within the limit of experimental error with C(1)-C(2) = 1.411 (6) Å and C(2)-C(3) = 1.408 (6) Å. The C(2)-C(2') bond connecting the allyl groups is 1.484 (6) Å. The bis-allyl molecule is inclined at 18.0° to the plane of the cyclopentadienyl ring, Figure 6.

Dahl and Wei<sup>1</sup> were the first to discuss the possibility of incomplete delocalization of bonds in cyclopentadienyl complexes. They found that one C-C (ring) bond in a  $\pi$ -cyclopentadienyl-Ni-norbornadiene ester complex  $[C_5H_5 \cdot Ni \cdot C_5H_5C_2(CO_2CH_3)_2]$  appeared to be longer (1.472 Å) than the other four which ranged from 1.375 to 1.433 Å. The variation in C(5) ring C-C bonds and in Ni-C distances led them to suggest an explanation in terms of the tendency of the Ni(II) ion to achieve a square planar configuration using  $d_{sp^2}$  hybrids. Bennett, Churchill, Gerloch, and Mason<sup>2</sup> and Gerloch and Mason<sup>13</sup> reported evidence of incomplete localization of bonds in  $\pi$ -cyclopentadienyl complexes lacking cylindrical symmetry. They explained the partial localization of the bonds in terms of the removal of the cylindrical symmetry around the metal ion resulting in the removal of the metal orbital degeneracy, which in turn serves to remove the degeneracy of the bonding orbitals on the cyclopentadienyl ring. They suggested that the structure of the  $\pi$ -cyclopentadienyl ring in this case should be formally written as indicated in Figure 5a. A reexamination<sup>14</sup> of the data for dihydrido- $\pi$ -cyclopentadienylmolybdenum indicated that these data do not support the reported<sup>13</sup> difference in carbon-carbon bond lengths. A number of the other  $\pi$ -cyclopentadienyl transitional metal complexes lacking in cylindrical symmetry have since been reported in which

(13) M. Gerloch and R. Mason, *J. Chem. Soc.*, 296 (1965).(14) S. C. Abrams and A. P. Ginsberg, *Inorg. Chem.*, **5**, 500 (1966).

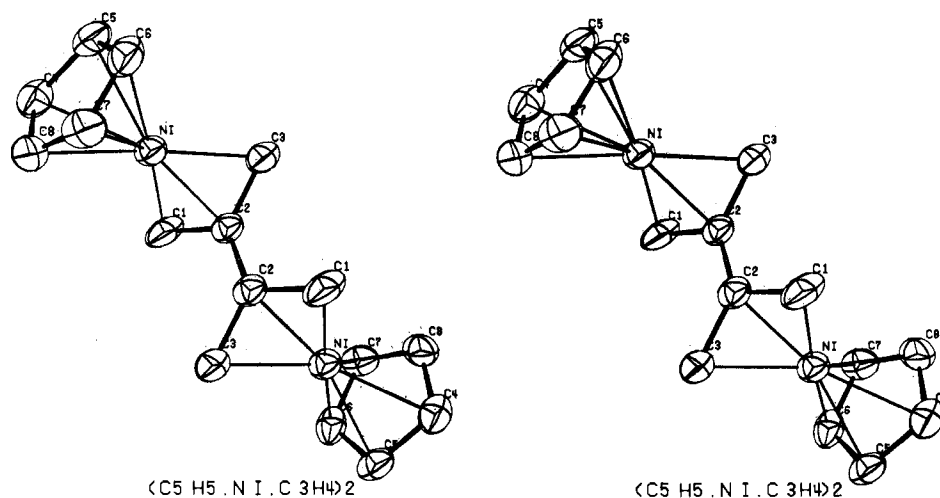


Figure 4.—ORTEP stereoscopic drawing of  $(C_5H_5 \cdot Ni \cdot C_3H_4)_2$  50% probability ellipsoids. For clarity no hydrogen atoms are included.

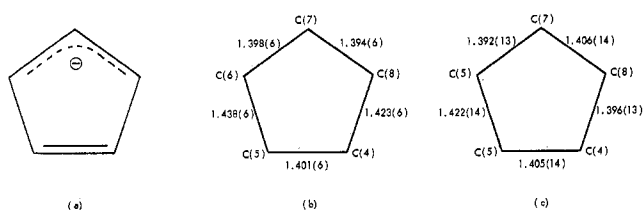


Figure 5.—(a) Postulated electron localization in  $\pi$ - $C_5H_5$  complexes lacking in cylindrical symmetry. (b) (c) Bond distances in  $C_5H_5$  ring. (b) Graphite monochromator Mo  $K\alpha$ . (c) Zr-filtered Mo  $K\alpha$ .

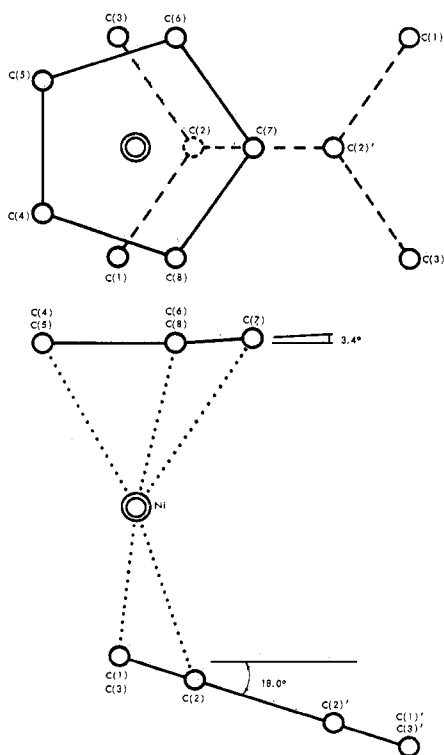


Figure 6.—Plan and elevation of complex showing inclination of bis-allyl group to  $C_5H_5$  plane.

partial localization of  $\pi$  electrons has been inferred.<sup>15</sup> In a recent review of these  $\pi$ -cyclopentadienyl complexes<sup>15</sup> it is concluded, however, that there is a ques-

(15) P. J. Wheatly, *Perspect. Struct. Chem.*, **1**, 23 (1967).

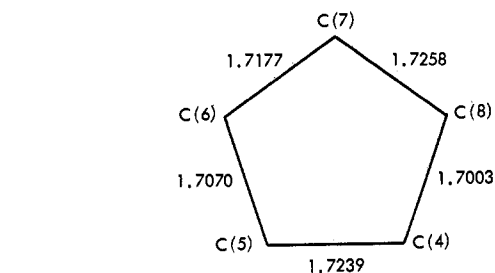


Figure 7.—Mulliken population analysis.

tion as to whether such distortions have indeed been detected.

The difference between the mean of the two short "allyl" bonds in the C(5) ring and the mean of the two "long" bonds  $1.431 - 1.396 \text{ \AA} = 0.035 \text{ \AA}$  which is  $\sim 5\sigma$  (Figure 5b). These results therefore, indicate that partial localization of the ring electrons has occurred with the formation of an "allyl" fragment and a short bond separated by two "long" bonds such as that predicted by Bennett, *et al.*,<sup>2</sup> and shown in Figure 5a. There is also some chemical evidence in the case of nickelocene that suggests it reacts as though an "allyl" fragment is involved. For example, nickelocene reacts with substituted acetylenes as though through the 1,3 addition of an allyl fragment.<sup>16</sup>

Extended Hückel molecular orbital calculations were also carried out on this complex by a semiempirical LCAO-MO method.<sup>17,18</sup> The procedure followed was similar to that of Schachtschneider, *et al.*<sup>18</sup> For convenience in computation, only one-half of the molecule was used in the calculation. Only one allyl group was used and the connecting carbon atom of the biallyl group replaced with a hydrogen ( $C_5H_5 \cdot Ni \cdot C_3H_5$ ). Two cases were considered: (1) The actual configuration observed with unequal carbon-carbon bonds in the  $C_5H_5$  ring. (2) The same configuration but with all the ring C-C bonds equal to  $1.423 \text{ \AA}$  and a planar  $C_5H_5$  ring.

The sums of the overlap populations for the cases

(16) M. R. Churchill and R. Mason, *Advan. Organometal. Chem.*, **5**, 119, (1967).

(17) M. Wolfsberg and L. Hemholz, *J. Chem. Phys.*, **20**, 837 (1952).

(18) J. H. Schachtschneider, R. Prins, and P. Ros, *Inorg. Chim. Acta*, **1**, 462 (1967).

of unequal and equal bonds are 12.4354 and 12.4259, respectively, which indicates the observed configuration with unequal bonds is more stable. A Mulliken population analysis for the case of equal bonds shows there is a tendency to reduce the number of electrons on bonds which were observed long and to add electron density to bonds which were observed short, Figure 7. The MO calculations, therefore, are in agreement with the observed partial localization of the bonds in the cyclopentadienyl ring.

**Acknowledgment.**—The author is indebted to Dr. J. H. Schachtschneider for help with the MO calculation and for the use of his MO programs, and to Dr. W. Keim for the preparation of the complex and for useful discussions. He is also indebted to W. F. Birka for aid with some of the calculations.

### Appendix

The intensities of reflections taken with Zr-filtered molybdenum radiation at low  $2\theta$  may be in error by significant amounts if collected on an automatic diffractometer without special precautions. This is illustrated in Figure 8, in which a  $2\theta$  scan along the (00 $l$ )

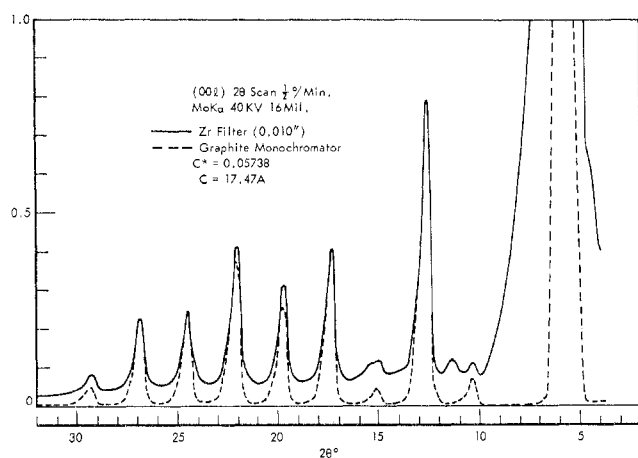


Figure 8.— $2\theta$  scan with graphite monochromatized and Zr-filtered Mo  $K\alpha$  radiation.

zone of a spherical crystal of  $[C_5H_5PNi(CO)_2]_2$ ,  $C = 17.47 \text{ \AA}$ , is shown taken with a graphite monochromator and with Zr-filtered Mo  $K\alpha$  radiation. The intensities were adjusted to the same relative scale. The much larger background and the presence of some  $\beta$  radiation in the Zr-filtered radiation, particularly for high in-

tensity reflections at low  $2\theta$ , is apparent. Uncertainties in the background corrections can be the major source of error in integrated intensity measurements at low  $2\theta$  for the data collected with Zr-filtered radiation by  $2\theta$  scan methods on automatic diffractometers. The systematic error is larger for crystals having large mosaic spread. In general, the mosaic spread for metal-organic and most organic crystals is larger than for inorganic crystals. The  $F$  values, *i.e.*, the intensities after correction for background, Lorentz-polarization, and absorption for the more intense low  $2\theta$  ( $\sin \theta/\lambda \gtrsim 0.20$ ) reflections for the graphite and LiF monochromatized and Zr-filtered radiation are compared in Table VII. Although the graphite and LiF

TABLE VII  
COMPARISON OF  $F$  VALUES FOR MONOCHROMATIZED  
AND Zr FILTERED Mo  $K\alpha$  RADIATION AT LOW  $2\theta$   
FOR THE  $(C_5H_5 \cdot Ni \cdot C_5H_4)_2$  COMPLEX

$hkl$	$\sin \theta/\lambda$	Graphite monochromator	LiF monochromator	Zr filter
$\bar{1}11$	0.090	124.47	122.41	73.59
200	0.108	127.19	128.41	35.41
$\bar{2}00$	0.108	127.99	128.67	36.52
002	0.112	113.89	112.55	32.12
$\bar{2}11$	0.121	71.75	71.04	53.55
$\bar{2}02$	0.125	77.80	79.40	75.23
012	0.129	68.79	70.36	63.87
$\bar{1}03$	0.157	79.32	82.41	77.02
202	0.180	79.46	82.57	78.67
103	0.193	87.31	92.22	84.94
$\bar{4}02$	0.205	71.40	71.96	67.37

data are in good agreement, the Zr-filtered data are generally lower for the more intense reflections below  $\sin \theta/\lambda \sim 0.20$  ( $2\theta \sim 16^\circ$ ).

Unfortunately, it is just at this range of  $2\theta$ , where the greatest error in intensity measurements with Zr-filtered Mo radiation occurs, that the larger percentage contribution to scattering for light atoms such as C, N, and H also occurs. As a result, the error in bond distances for light atoms such as a C-C bond, particularly in the presence of heavy atoms, will be greater if Zr-filtered radiation rather than monochromatic radiation is used. The bond distances in the cyclopentadienyl ring determined with the graphite and Zr-filtered data are compared in Figures 5b and 5c. Although the weights of the more intense low-angle reflections were deliberately reduced for the latter data during the least-squares refinement, the estimated standard deviations in C-C bond distances in the C(5) ring are more than twice as large as those obtained with graphite monochromatized data.